Adsorption of random copolymer on surfaces

F. Aguilera-Granja, Ryoichi Kikuchi

▶ **To cite this version:**

F. Aguilera-Granja, Ryoichi Kikuchi. Adsorption of random copolymer on surfaces. Journal de Physique II, 1994, 4 (10), pp.1651-1675. 10.1051/jp2:1994223 . jpa-00248068

HAL Id: jpa-00248068
https://hal.science/jpa-00248068

Submitted on 4 Feb 2008

HAL is a multi-disciplinary open access archive for the deposit and dissemination of scientific research documents, whether they are published or not. The documents may come from teaching and research institutions in France or abroad, or from public or private research centers.

L'archive ouverte pluridisciplinaire **HAL**, est destinée au dépôt et à la diffusion de documents scientifiques de niveau recherche, publiés ou non, émanant des établissements d'enseignement et de recherche français ou étrangers, des laboratoires publics ou privés.

J. Phys. II France **4** (1994) 1651–1675 OCTOBER **1994**, PAGE 1651

Classification
Physics Abstracts
05.20 – 05.50 – 82.65D – 61.25H – 82.20W

Adsorption of random copolymer on surfaces

F. Aguilera-Granja ([1]) and Ryoichi Kikuchi ([2])

([1]) Instituto de Física "Manuel Sandoval Vallarta", Universidad Autónoma de San Luis Potosí, San Luis Potosí, S.L.P. 78000, México
([2]) Department of Materials Science and Engineering, University of California, Los Angeles, CA 90024-1595, U.S.A.

(Received 2 December 1993, revised 27 May 1994, accepted 13 July 1994)

Abstract. — The conformations adopted by random copolymers of two components adsorbed on a flat surface are studied by the use of a simulation technique. The simulation technique is based on the analytical equilibrium calculation of the Cluster Variational Method and is a generalization of the Cluster Growth Probability Method to the case when the probabilities include chemical bonds. The model used here assumes that the two copolymer components have different interaction energies with the surface. The changes in the physical and geometrical properties are studied as a function of the copolymer length and the interaction energies with the surface. The configuration of the adsorbed copolymers depends strongly on the interactions with the surface. The behavior of the copolymers shows some similarities with homopolymers, but also some differences are shown. The results shown here can be regarded as a guideline for controling some specific configurations adopted by the adsorbed copolymers on colloid particles.

1. Introduction.

Spatial properties of adsorbed polymers have been the subject of numerous experimental and theoretical studies [1-30]. However, most of the time the homopolymers are the main subject of theoretical work [11-20]. It has been only very recently that the study of polymer adsorption has treated polymers with a much more complex architecture than the simple homopolymers [21-30]. Many of the theoretical studies are based on numerical simulations due to the difficulties of the analytical techniques to formulate statistical treatment that is able to represent polymers with complex structures like polymers with lateral branches, comb like polymers, star like polymers and copolymers with long alternating sequence of components and block copolymers [21-30]. Another advantage of the simulation technique is that it provides us with a physical representation of the system not only at the surface but also on the subsequent planes parallel to the surface. With the simulation we can visualize systems that otherwise will be practically imposible to see in laboratories. The understanding of the role that the

architecture of the complex polymers plays in the adsorption will ultimately indicate us how to design the polymers so that we can get the optimal polymer conformations for applications like the steric stabilization and the adhesion.

The random copolymers of different components are of interest due to the fact that different segments (monomers) which are used in building (synthesizing) copolymers can have different properties, and hence they may see the surface, on which the copolymers are adsorbed, in very different ways. For instance in a random copolymer made of two different kinds of segments ($\mathcal{A}$ and $\mathcal{B}$) in an aqueous solvent, the $\mathcal{A}$ segments may have affinity to the surface (hydrophobic), while the $\mathcal{B}$ segments may have repulsion from the surface (hydrophilic). This different behavior in the polymer segments opens the possibility to control the type of configurations of the adsorbed polymers by changing their affinities to the surface. This property is expected to allow us to design copolymers for required specific configurations and as a consequence to control the interaction between colloidal particles coated with polymers. For an extensive review of the polymer adsorption problem the reader may consult the review papers by Takahashi [5], Fleer [17] and Pincus [30] as well as references quoted therein.

In the present paper, we study a type of random copolymers built of two types of segments in an aqueous solvent, the hydrophobic $\mathcal{A}$ segments and the hydrophilic $\mathcal{B}$ segments. We focus our attention in the change of configurations of the adsorbed copolymers as a consequence of the change of the surface affinity of one of the segments ($\mathcal{B}$). Particularly, we choose for our study the layer thickness of the adsorbed copolymers and the area covered by them in the adsorption process. We pay special attention to these properties because it is generally belived that in the steric stabilization of the colloidal particles, these two properties play predominant roles. In addition, we also study other geometrical properties like fractions in the trains, tails and loops as well as the average number of tails of these linear copolymers. The polymer concentration in the solution (bulk) we work with is 1%, the parameter we use for the average bulk lenth is L = 44 [18, 19, 31, 32], and the system size used in the simulation is $50 \times 50 \times 20$ lattice points. The length of a copolymer generated by the simulation is denoted by ℓ. The energy unit we use is $k_{\mathrm{B}}T$.

2. Model and method.

Before we start the simulation, the equilibrium state of the copolymers close to the surface is to be determinated using the Cluster Variational Method (CVM) [33, 34]. This is to calculate the analytical input for the simulation [18-21]. Since the method and all the details about the way in which the analytical calculation and the simulation are done can be found elsewhere [18, 19], we simply highlight the important points of this method.

2.1 ANALYTICAL INPUT. — In the present case, we use the pair approximation of the CVM in the simple cubic lattice [18, 19, 31, 32]. The lattice planes parallel to the substrate are numbered by n, $n = 1$ being the first plane closest to the substrate (solid surface). The configurational probabilities of a lattice point (the single site probabilities) in the plane n are written as $x_{n;i}$, for a solvent ($i = -1, 0$), for an end copolymer segment ($i = 1, 2, 3$), for an $\mathcal{A}$ copolymer segment or hydrophobic monomer ($i = 4, 5, 6, 7$) and for a $\mathcal{B}$ copolymer segment or hydrophilic monomer ($i = 8, 9, 10, 11$). This is listed in table I, where all species and their statistical weights in the case of a simple cubic lattice are shown [18-19]. A polymer segment has connecting bonds. A pair of adjacent segments are either connecting or non-connecting. When they are in the same plane n, their probabilities are written as $y^{(a)}_{n;i,j}$ and $y^{(b)}_{n;i,j}$ for connecting and non-connecting, respectively. For pairs perpendicular to the substrate, when the segment i is on the plane n and j on $n + 1$, their probabilities are written as $z^{(a)}_{n+h;i,j}$

Table I. — *Definition of the subscript i and the statistical weight factors for the single site probabilities for the simple cubic lattice used in our model. The surface is located in the down direction. The horizontal bonds are parallel to the surface, and the vertical bonds are perpendicular to it.*

Definition of the subscript i and the weights ω_i		
Species and Connections	i	ω_i
Solvent molecule (m)	-1	1
Solvent molecule (m)	0	1
End monomer (e)	1	1
(e)–	2	4
(e)	3	1
Hydrophobic monomer (A)–	4	4
–(A)–	5	6
(A)	6	1
(A)–	7	4
Hydrophilic monomer (B)–	8	4
–(B)–	9	6
(B)	10	1
(B)–	11	4

and $z^{(b)}_{n+h;i,j}$ (with $h \equiv 1/2$, and hence $n+h$ being the middle point of the two planes). The probabilities on the plane $n = 1$ need special attention; because a chemical bond cannot point downward toward the solid surface, the probabilities with bonds pointing toward the surface are zero. The number of equivalent configurations due to the different type of pairs (connecting and non-connecting) are listed in tables II and III; those pairs not shown in the tables are zero. In the simulation, it is important to point out that each configuration of the connecting arm is treated as distinguishable [19, 32].

The energy of the system is made of two contributions. The two energy parameters that control the surface-polymer interactions used here are denoted by $\varepsilon^{(1)}$ and $\varepsilon^{(2)}$, in which $\varepsilon^{(1)}$ is the hydrophobic attraction of an $\mathcal{A}$ segment to the surface and $\varepsilon^{(2)}$ the hydrophilic repulsion

Table II. — *(a) The statistical weight factors for the connecting pairs within the same plane* ($w^{(a)}_{y;i,j}$). *For the first layer* $n = 1$ *the statistical weight vanishes when* i *or* j *is 4 or 8. (b) The statistical weight factors for the connecting pairs between planes* ($w^{(a)}_{z;i,j}$). *For the first layer* $n = 1$ *the statistical weight vanishes when* i *is 6 or 10. Those pairs* (i, j) *not shown in the tables are zero. The subscripts* y *and* z *indicate the direction of the bond;* y *for horizontal* (i.e., *parallel to the solid surface) and* z *for vertical, respectively.*

$i \quad \backslash \quad j$	2, 8, 11	4, 7	5	9
2, 8, 11	0	1	3	0
4, 7	1	1	3	3
5	3	3	9	9
9	0	3	9	0

a)

i on n $\backslash$ j on $(n+1)$	1, 10	4	6	8
3, 10	0	4	1	0
6	1	4	1	4
7	4	16	4	16
11	0	16	4	0

b)

Table III. — *(a) The statistical weight factors for the non-connecting pairs within the same plane* ($w^{(b)}_{y;i,j}$). *For the first layer* $n = 1$ *the statistical weight vanishes when* i *or* j *is 1, 4, 6, 8 or 10. In (b) the statistical weight factors for the non-connecting pairs between planes* ($w^{(b)}_{z;i,j}$). *For the first layer* $n = 1$ *the statistical weight vanishes when* i *is 1, 4 or 8. Those pairs* (i, j) *not shown in the tables are zero. The subscript* y *indicates the horizontal direction, and* z *the vertical.*

$i \quad \backslash \quad j$	-1, 0, 1, 3, 6, 10	2, 4, 5, 7, 8, 9, 11
-1, 0, 1, 3, 6, 10	1	3
2, 4, 5, 7, 8, 9, 11	3	9

a)

i on n $\backslash$ j on $(n+1)$	-1, 0, 3	2, 7, 11	5, 9
-1, 0, 1	1	4	6
2, 4, 8	4	16	24
5, 9	6	24	36

b)

of a $\mathcal{B}$ segment from the surface. The surface-polymer interaction in our model can be written as follow:

$$\varepsilon^{(i)} = \begin{cases} \varepsilon^{(1)} & \text{for the hydrophobic segments or } \mathcal{A} \ (i = 1, 2, 3, ...7), \\ \varepsilon^{(2)} & \text{for the hydrophilic segments or } \mathcal{B} \ (i = 8, 9, 10, 11). \end{cases} \quad (1)$$

The interactions in equation (1) are extended to the segments on $n = 1$ only as is shown in figure 1. Notice that in this model we assume that the end segments are of the $\mathcal{A}$ type. The convention for the energy parameters is that they represent attraction when they are positive

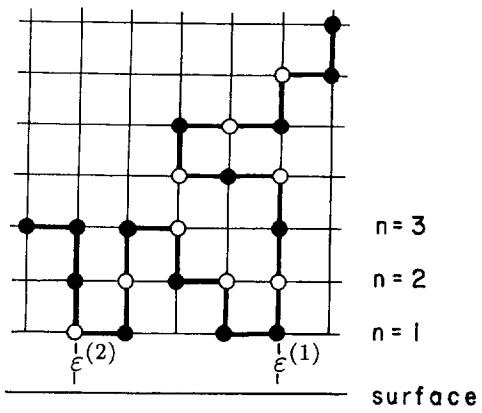

Fig. 1. — Two-dimensional representation of the model used in this simulation. Black segments correspond to $\mathcal{A}$ or hydrophobic segments, while white ones correspond to $\mathcal{B}$ or hydrophilic segments. This figure also illustrates the energies of interaction with the surface used in this model. $\varepsilon^{(1)}$ is the interaction energy of an $\mathcal{A}$ segment, and $\varepsilon^{(2)}$ is the interaction energy of a $\mathcal{B}$ segment.

and repulsion when negative. The energy of the system based on this convention can be written as follow:

$$E = -L\sum_{i=1}^{11}\varepsilon^{(i)}w_i x_{1,i}\ , \tag{2}$$

where $x_{1,i}$ ($i = 1, 2.., 11$) is the probability to find a copolymer segment i on the plane $n = 1$ and L is the number of lattice points within a plane parallel to the solid surface. Notice that the energy contribution from $x_{1,i}$ for $i = 1, 4$ and 8 vanishes due to the fact that such probabilities are not allowed on the plane $n = 1$.

The entropy of the system is written in the pair approximation of the CVM for the simple cubic structure as [18, 19, 31, 32]:

$$\begin{aligned} S \;=\; k_{\mathrm{B}}\,L\sum_{n}\Bigg\{ & 2+5\sum_{i\,=\,0}^{11} w_i\,\mathcal{L}(x_{n,i}) \\ & -2\sum_{i,j}\Big[w^{(a)}{}_{y,i,j}\,\mathcal{L}(y^{(a)}{}_{n;i,j}) + w^{(b)}{}_{y;i,j}\,\mathcal{L}(y^{(b)}{}_{n;i,j})\Big] \\ & -\sum_{i,j}\Big[w^{(a)}{}_{z,i,j}\,\mathcal{L}(z^{(a)}{}_{n+h;i,j}) + w^{(b)}{}_{z;i,j}\,\mathcal{L}(z^{(b)}{}_{n+h;i,j})\Big]\Bigg\}\ , \end{aligned} \tag{3}$$

where the w_i, $w^{(\nu)}_{y,i,j}$, $w^{(\nu)}_{z,i,j}$ are the statistical weight factors (number of equivalent configurations) of the single site probabilities ($x_{n,i}$), pair probabilities within the same plane ($y^{(\nu)}_{n;i,j}$) and pair probabilities between plains ($z^{(\nu)}_{n+h;i,j}$) as shown in tables I, II and III, respectively. The function $\mathcal{L}(x)$ is defined as $x\ln x - x$ [31]. This expression reduces to the case of the bulk formula when the variables do not depend on n [31].

The equilibrium distribution of the system is calculated from the minimization of the grand potential Ω with respect to the pair probabilities for given values of the interaction energies,

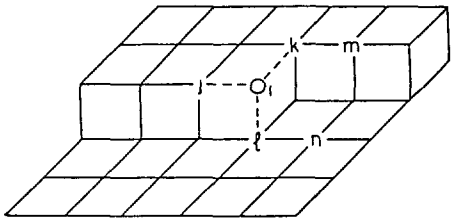

Fig. 2. — An intermediate stage of the construction of the simple cubic lattice used in our simulation model.

the temperature T, the copolymer length L, and the chemical potential values. The grand potential Ω can be written as follows:

$$\Omega = E - TS - L\sum_{n,\imath}\mu_\imath\rho_{n,\imath} \,, \tag{4}$$

where E is the internal energy defined in equations (1) and (2), S the entropy as in equation (3), $\mu_\imath$ the chemical potential and $\rho_{n,\imath}$ the density of the i^{th} species on the plane n. After all the cluster equilibrium distributions ($\{x_{n,\imath}\}$, $\{y^{(\nu)}_{n;\imath,\jmath}\}$, $\{z^{(\nu)}_{n+h;\imath,\jmath}\}$) are known we can proceed with the simulation.

2.2 SIMULATION PROCEDURE. — When all the cluster probabilities of the system are know, we are ready to begin the simulation process using the Crystal Growth Probability Method (CGPM) [32, 34]. Although we use the same information contained in the output of the analytical CVM, the CGPM simulation reveals the information that is not demonstrably available in the analytical results. In order to make the presentation concrete, we explain the simulation method based on the pair approximation for the simple cubic lattice. The simulation procedure is done as follows: we construct the system from bottom to top beginning next to the substrate, from left to right, and from back to front, by placing a species at a lattice point one at a time. Let us suppose that the lattice has been built up to the edge formation $j-k-l-m-n$ in figure 2, and the next one to be placed is i. Around the i point, three out of the total six nearest neigbours have been placed and known. We can show that the nature of correlation in the pair approximation is equivalent to writing the probability for placing i in the superposition form [32, 34] as

$$P_{4,n}(i,j,k,l) = y_{n;\jmath\,\imath}\, y_{n;k\,\imath}\, z_{n-h;l\,\imath} \,/\, (x_{n;\imath})^2 \tag{5}$$

The subscripts in the probability $P_{4,n}$ indicate the number of points in the cluster (4) and the plane number (n), respectively. The expression in equation (5) contains an inherent approximation due to the nature of the CVM [32, 34].

Starting with the probability expression $P_{4,n}(i,j,k,l)$, we can proceed to formulate our basic relations for this simulation. When j,k, and l are known, the conditional probability $\wp_n(i;j,k,l)$ of placing the species i at the circled point in figure 2 is defined as

$$\wp_n(i;j,k,l) = P_{4,n}(i,j,k,l) \,/\, \sum_m P_{4,n}(m,j,k,l) \,. \tag{6}$$

This holds for $n \geq 2$. For the first plane $n = 1$ next to the surface, we use a relationship similar as equation (5) without the point l. We construct the lattice beginning from the surface in

such a way that the conditional probabilities are satisfied at every point. We use a random number to choose the probabilities to be placed in each one of the lattice points. This is the general recipe of our CGPM simulation based on the CVM pair approximation. However, with this type of simulation, it is required to construct the simulation pattern many times to avoid bias in the different statistical patterns [19, 32, 34].

In the present polymer simulation, we need a special constraint to take care of the direction of chemical bonds, as was done for the case of polymers in the solution [32]. It can occur in figure 2 that m and n are polymer segments and their bonds are going through another segment at h (next corner to be formed). In this case, we cannot place at i a polymer segment with a bond directed towards h. In order to avoid such conflict, in choosing a species to be placed at i, we need information not only for the three nearest-neighbor points j, k and l but also for two more points m and n. In short we can say that we are working with a pseudo-six-point cluster $i - j - k - l - m - n$ [32]. Similar consideration is also needed for the surface point.

The system size used in this simulation is $50 \times 50 \times 20$ lattice points, and the system is truncated in five of the six faces. Because of the truncation of the system, some polymers near the truncation surface have only one ending point inside the simulation field. For the sake of simplicity, when the statistical count is done these polymers are disregarded. Another anomaly of this simulation is the existence of closed loops of polymers, which are also disregarded in the statistical counting. The probability of closed loops decreases when bigger clusters are used [32].

We postulate the following rules on distribution of the $\mathcal{A}$ and $\mathcal{B}$ segments inside copolymers. The edges (head and tail) are segments of type $\mathcal{A}$, and the segment next to an edge is also an $\mathcal{A}$. For the internal segments the rules are that $\mathcal{A}$ may sit next to $\mathcal{A}$ or $\mathcal{B}$, and $\mathcal{A}$ always comes after $\mathcal{B}$, or in other words no two $\mathcal{B}$'s are allowed to sit next to each other. In polymers generated by the simulation, $\mathcal{A}$ and $\mathcal{B}$ are almost alternated when the $\mathcal{A}$ fraction is equal to the $\mathcal{B}$ fractions, but in any other concentration the distribution is almost random. In the present work, the $\mathcal{B}$ fraction (α = *number of $\mathcal{B}$ segments in a chain/number of all internal segments in a chain)* depends on the polymer length because of these rules. The dependence of the $\mathcal{B}$ fraction (α) in this simulation is shown in figure 3. The $\mathcal{B}$ fraction for long polymer chains is 0.48.

The average length of a copolymer in our paper for the analytical calculations is specified by the ratio of the total number of segments to a half of the number of end segments [31]. In the case of the average bulk length L, this ratio is calculated far away from the surface (in the bulk). In this paper L is fixed at 44 in the plane $n = 20$ [18, 19, 31, 32], which is assumed to be close to the bulk. The L value can be changed by changing the number of end segments which are controlled by the chemical potential associated with the end segments.

The sample of the polymers generated by this simulation method is a polydisperse sample [18, 19, 32], which is made of copolymers with a length (ℓ) distribution as will be illustrated later in figure 8. In the simulation the average length of the generated distributions (Fig. 8) can be changed by varying the L in the analytical results.

3. Results.

3.1 ANALYTICAL RESULTS. — We present some of the analytical results of the CVM on which our simulation is based in figures 4, 5, 6 and 7. In figure 4a, we see the density profile as a function of the distance from the surface, for a fixed $\varepsilon^{(1)} = 2.0$ and three different $\varepsilon^{(2)}$ (=0.0 circle, -1.0 square, -2.0 triangle). For the sake of simplicity, we call these three cases CRL for circle, SQR for square, and TRI for the triangles. We keep these definitions throughout the paper unless otherwise specified. The density profile of polymers decreases monotonically and

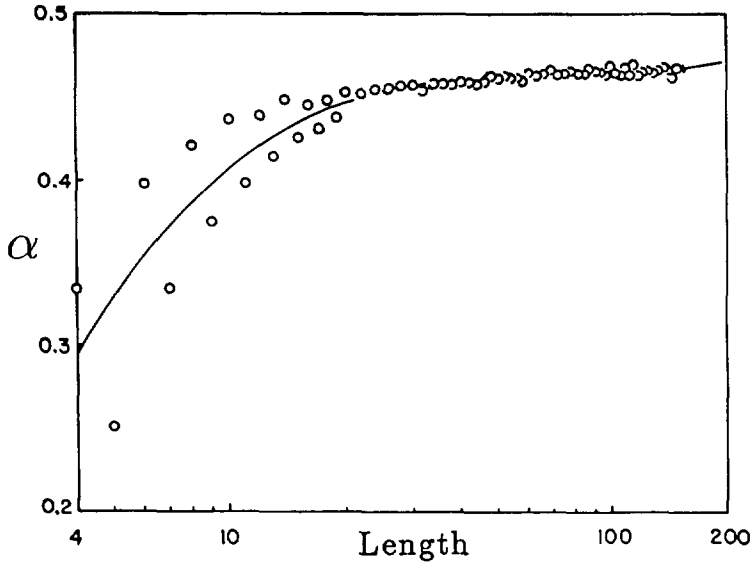

Fig. 3. — The $\mathcal{B}$ fraction (α = *number of* $\mathcal{B}$ *segments in a chain / number of all internal segments in a chain*) of the copolymers generated by this simulation as a function of the polymer length (ℓ). The continuous line is an aid to the eye.

approaches the bulk value as we move away from the surface. We found that near the surface the profiles depend strongly on the surface interactions as have been pointed out by de Gennes and Pincus [35, 36]. Our density profiles presented here are in qualitatively good agreement with those reported by Balazs and coworkers for random and alternating copolymers [25]. It is also relevant to mention that some calculations on the density profiles for random copolymers with a few stickers (low α) by Marques and Joanny predict an exponential decay for the penetrable wall case [37]. However in our case (high α) we did not find a simple function that describes the density profiles. The surface coverage θ and the adsorbed amount of polymers Γ_{exc} (as defined by Roe) [11] decrease as the repulsion felt by $\mathcal{B}$ segments increases. The surface coverage in these cases are 0.61, 0.318 and 0.0705 for CRL, SQR and TRI, respectively. The adsorbed amount Γ_{exc} changes from 0.95 for the CRL, 0.59 for SQR and finally 0.164 for the TRI case. It is worth mentioning that the TRI case shows that some polymers are adsorbed on the surface even when the average attraction is zero. The reason is that the last two segments at an edge of a copolymer always feel attraction from the surface. The percentage of end segments as a function of the distance from the surface is shown in figure 4b. The probability to find the end segments close to the surface increases as the repulsion to the $\mathcal{B}$ segments increases. The high percentage of end segments close to the surface in the TRI and SQR cases implies that as the repulsion increases it is less probable to find long chains close to the surface, since longer chains have a larger fraction of $\mathcal{B}$ segments and hence feel stronger repulsion from the surface.

In the homopolymer case there is a critical energy below which there are not adsorbed polymers [18] as Binder and coworkers found in analogy with a semi-infinite magnetic systems [38]. However, in the copolymer case due to the existence of two energy parameters there is a curve of critical values. For a more extensive review the reader may consult references [18, 38] and references quoted therein.

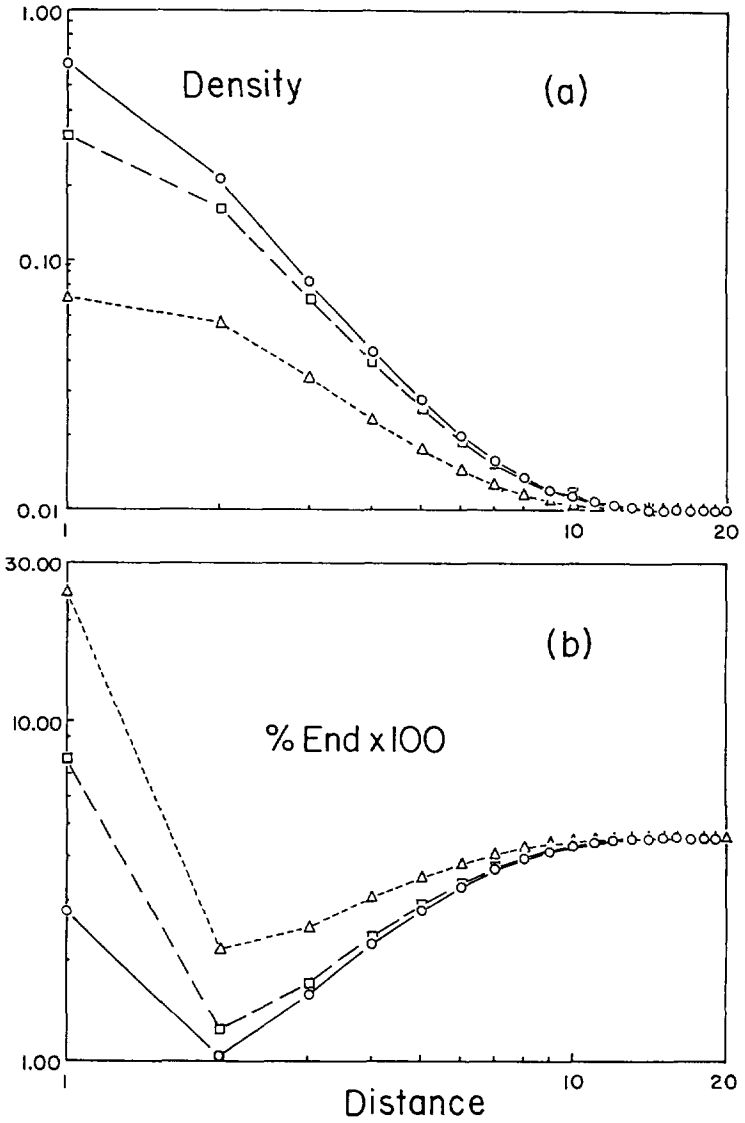

Fig. 4. — Analytical results used as an input in this simulation: (a) the density profiles and (b) percentage of end segments, as functions of the distance from the surface for a fixed $\varepsilon^{(1)} = 2.0$ and different $\varepsilon^{(2)}$ (=0.0 circle, -1.0 square, -2.0 triangle). In the analytical results α is fixed at 0.48 in the plane $n = 20$. The marks correspond to calculated points.

For polymers within a semi-infinite system the presence of the surface itself induces anisotropic behavior regardless of the surface interaction that is present in the polymer adsorption problem. We illustrate this anisotropic behavior in figure 5. In (a) we calculate the ratio of the parallel polymer bonds to the perpendicular polymer bonds as a function of the distance from the surface ($\sum^{*} w^{(a)}_{y;i,j} y^{(a)}_{n;i,j} / \sum^{*} w^{(a)}_{z;i,j} z^{(a)}_{n+h;i,j}$, where * indicates all polymer segments). These results indicate that the polymers prefer the parallel direction near the surface. As the repulsion felt by $\mathcal{B}$ segments increases the system becomes more homogeneous near the

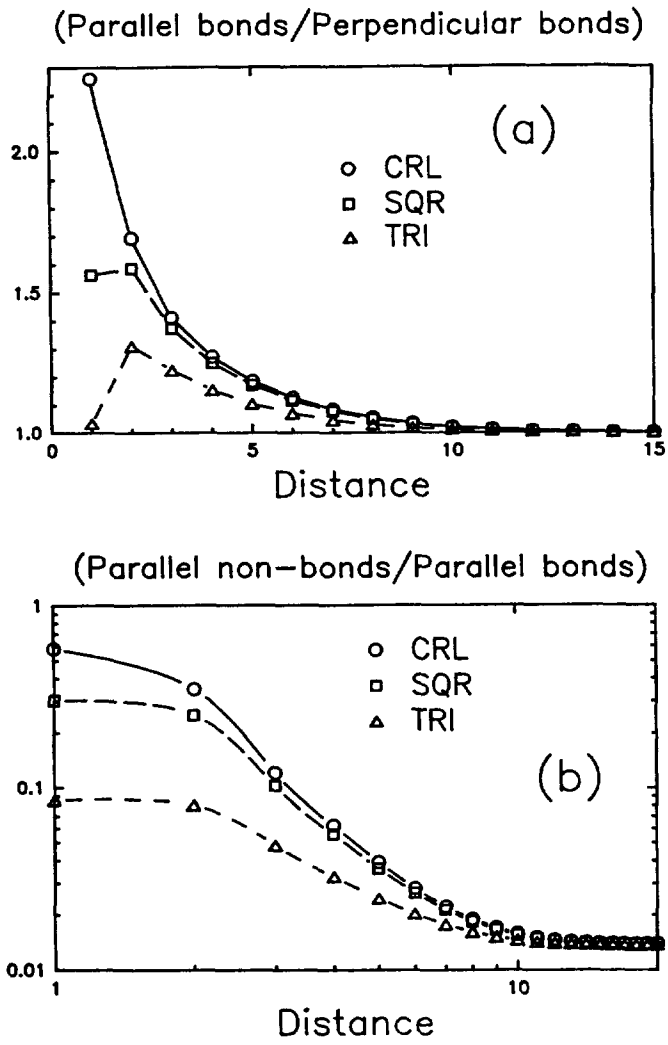

Fig. 5. — (a) Ratio of the pair of parallel polymer bonds to the pair of perpendicular bonds as a function of the distance form the surface. (b) Ratio of the parallel polymer pairs that are not connected to the parallel pairs that are connected as a function of the distance from the surface.

surface. It is worth noting that in the TRI case even when the average attraction is zero the system is still anisotropic, the reason of this being the entropy effect near the surface. In (b) we calculate the ratio of the parallel polymer pairs that are of no-bonds to those of bonds ($\sum^* w^{(b)}_{y;i,j} y^{(b)}_{n;i,j} / \sum^* w^{(a)}_{y;i,j} y^{(a)}_{n;i,j}$). This ratio is remarkably similar to the density concentration profile shown in figure 4a. We calculate the ratio of figure 4a to figure 5b and call it η, which is plotted in figure 6. We find that the curves for CRL, SQR and TRI are practically the same except the few planes near the surface.

In figure 4b we present the percentage of end segments as a function of the distance from the surface. Now we present the normalized end fraction as a function of the distance from the surface for the three different types of end segments we have in our model (species 1, 2

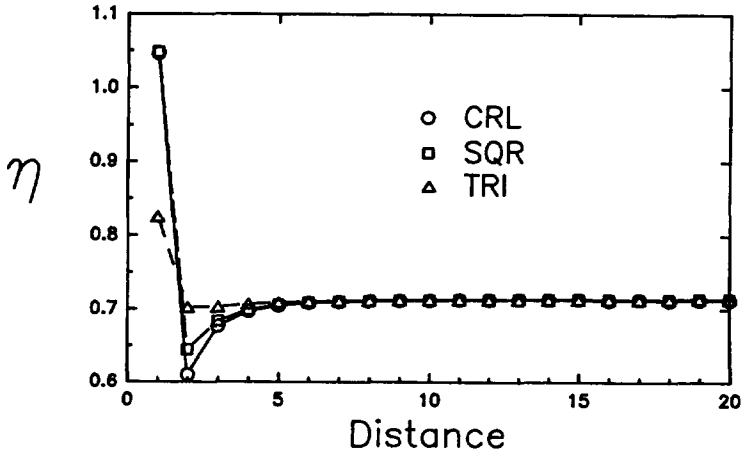

Fig. 6. — The ratio η of figure 4a to figure 5b as a function of the distance from the surface.

and 3 in Tab. I) in figure 7. The end segments whose arms are pointing toward the surface (downward direction) are represented by a triangle down (or "down "the for sake of simplicity), end segments with the arms pointing away upward from the surface (or "up ") are represented by a triangle up, and end segments with the arms parallel to the surface by a diamond (we present one of the possible four directions since all of them are equivalent). Notice that the fraction is normalized as $\bigtriangledown + 4\Diamond + \bigtriangleup = 1$ in every plane. Since the end-down segments are not allowed on the $n = 1$ plane, a big anisotropy in the down and up directions occurs. This anisotropy disappears approximately in ten planes away from the surface. The normalized end fraction is not very sensible to the change in the $\varepsilon^{(2)}$ surface interaction since for the three cases in figure 7 we have practically the same values. Far away from the surface the end fractions tend to 1/6 since all six possible directions are equivalent (in the case of a simple cubic lattice). For a more extensive discussion on the anisotropic behavior in the perpendicular and parallel directions, the reader may consult references [38] and [39].

3.2 SIMULATION RESULTS. — For homopolymers, it is well known theoretically [15, 19] and experimentally [2] that when the polymers are polydispersed, there is a preferential adsorption for longer chains. To examine the corresponding properties for random copolymers is one of the main purposes of this paper. The results of this simulation are shown in figure 8, where the adsorption probability as a function of the polymer length (ℓ) is shown. The distribution of the adsorbed copolymers shows a preference for shorter polymer chains as the repulsion of the $\mathcal{B}$ segments increases. This is a consequence of the low fraction of the $\mathcal{B}$ segments in short chains. The average length of the adsorbed polymers are $\ell_{\mathrm{CRL}} = 56$, $\ell_{\mathrm{SRQ}} = 40$, and $\ell_{\mathrm{TRI}} = 19$. The polydisperse indices [32] are $N_{\mathrm{CRL}} = 1.50$, $N_{\mathrm{SQR}} = 1.64$, and $N_{\mathrm{TRI}} = 1.36$. As a reference, the average length in the bulk (far away from the surface) is $\ell_{\mathrm{bulk}} = 22$.

Information about the conformation of the adsorbed copolymers and their changes with the energy of interaction can be inferred when we study the end-to-end distance. Examples of the possible end-to-end distance for two adsorbed polymers on a flat surface are illustrated in figure 9. The bulky configurations (more condensed) correspond to small values for the end-to-end, while the extended configurations present large values for this distance. This quantity for polymers in the solution in this type of simulations based on the CVM obeys a power law

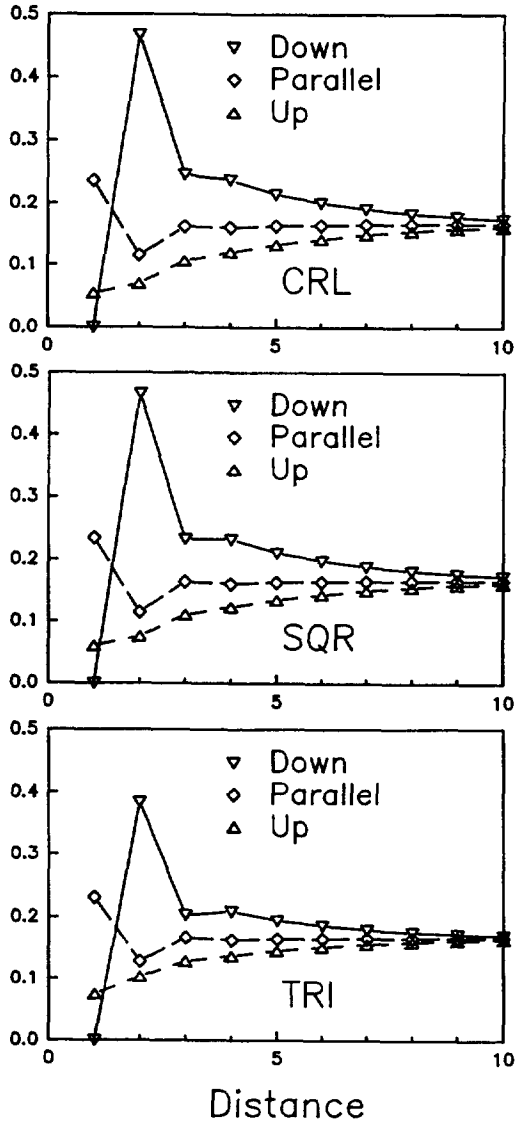

Fig. 7. — The normalized end fraction as a function of the distance from the surface for the three different types of end segments.

[32] as follow:

$$\langle |\mathbf{r}_1 - \mathbf{r}_2| \rangle = c\ell^{\nu} , \tag{7}$$

where c is a constant that depends on the model and ν is an exponent independent of the lattice model. This exponent ν may not necessarily correspond to the one calculated by Fisher [40] and de Gennes [41] ($\nu = 3/(d+2)$) as a function of the dimensionality of the system (d) for polymers in the bulk, due to the fact that the latter evaluation is for infinite length

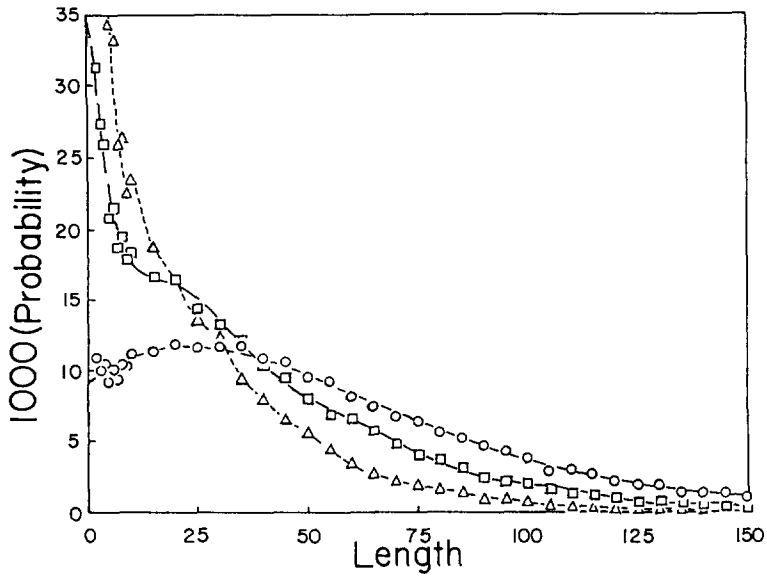

Fig. 8. — Distribution of the adsorbed copolymers, or adsorption probability, on the surface as a function of the polymer length (ℓ) for the same interaction energies as those in figure 4.

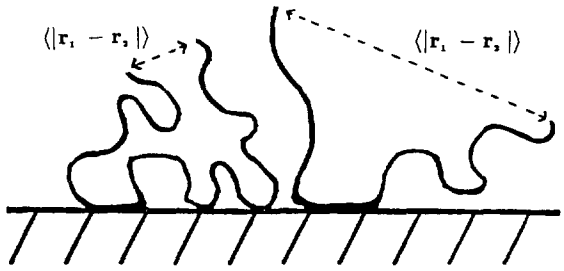

Fig. 9. — Illustration of two possible cases of the end-to-end distance for an adsorbed polymer on a flat surface. The short end-to-end distance indicates a coiled shape configuration while a large end-to-end distance indicates an extended configuration.

polymers while our evaluation of the ν is for finite length polymers close to the surface. The behavior of the ν in our simulation is useful to understand the change of the configurations as the interaction energy changes. In the case of copolymers adsorbed on a flat surface, it is clear that we do not have either a pure two-dimensional system nor a three-dimensional system, and hence if a power law as equation (7) is obeyed the ν exponent (ν_s) should be between the three-dimensional value (ν_{3d}) and the two-dimensional value (ν_{2d}): that is $\nu_{3d} \leq \nu_s \leq \nu_{2d}$. The result of the direct counting from this simulation are shown in figure 10. The exponents obtained here are $\nu_{CRL} = 0.64$, $\nu_{SQR} = 0.66$, and $\nu_{TRI} = 0.72$. The change in these exponent values means that the configurations of the adsorbed copolymers are of curly shape (bulky) for the small exponent, and extended for the large exponent. A typical extended configuration is the case in which the copolymer has one of the edges attached to the surface and the rest of the polymer body extend into the solution. As a reference we may mention that the ν exponent of the homopolymer case (when all segments feel the same energy) is 0.62 [19]. Although

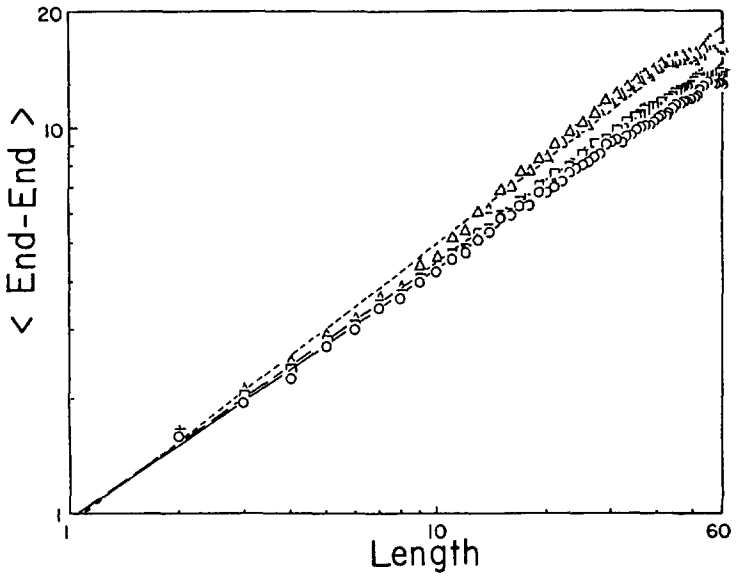

Fig. 10. — The end-to-end distance of the adsorbed copolymer as a function of the polymer length for the same interaction energies as those in figure 4.

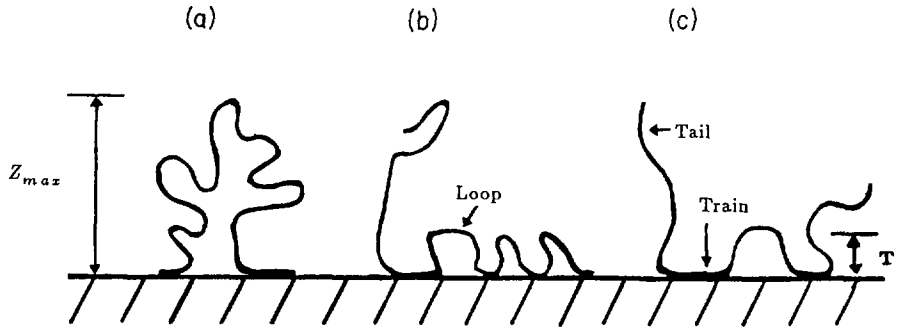

Fig. 11. — Illustration of the two definitions used to characterize the layer thickness of the adsorbed copolymers. Z_{max} gives information about the farthest segment of the adsorbed polymers as is illustrated in (a), (b) and (c), while the thickness T gives information about the average height of the loops formed by the adsorbed polymers as in (b) and (c). We also illustrate names for loop, train and tail.

the exponents found here for the CRL and the SQR are close to the homopolymer case, the conformations for the copolymers may be different from those of the homopolymers. It is to be noted that our simulation does not try to verify any asymptotic behavior for infinitely long copolymers, and that we rather present the relative behavior of the end-to-end distance for a limited range of lengths computed within the reasonably available CPU-time.

Before finishing this topic, it is worth pointing out that in this type of CVM simulations the volume exclusion is taken into account in two steps [19, 32]. The first step is that we avoid disallowed configurations by using a pseudo-six-point cluster as mentioned above [19, 32]. The second is that forbidden closed loop chains are discarded when we count chain configurations. These preventive steps make our simulation capable of taking into account

long-range correlations of the lattice statistics which are not incorporated in the original CVM pair approximation.

In order to study the differences in the conformations, we examine the layer thickness. The two definitions of the layer thickness we use here are illustrated in figure 11. The first one (shown in (a)) is called Z_{max}, and is related to the adsorbed copolymer segment located farthest from the surface. The second definition is called the thickness T and is related to the average height of the loops formed by the adsorbed copolymers as is illustrated by figures 11b and c. In the case of Z_{max} we proceed as follow: we record the largest n (layer) number of each of the adsorbed copolymer chains, for which the largest n may be at the end of the adsorbed polymer (Fig. 11c) or at an internal segment (Figs. 11a and b). The results are shown in figure 12a in the log-log scale. The Z_{max} shows a dependence on ℓ that seems more complex than a simple power law. The simulation results suggest the existence of two regions with the boundary located at $\ell \simeq 50$. The existence of two regions may be related with a change in the copolymer conformations with the length. Even when a simple power law ($c\ell^{\gamma}$) is not obeyed for the entire length range, it is interesting to compare the exponents when a power law is followed approximately. The values are $\gamma_{CRL} = 0.57$, $\gamma_{SQR} = 0.61$ and $\gamma_{TRI} = 0.66$. Comparison with the γ exponent in the homopolymer case ($\gamma = 0.50$) [19, 21] shows that the exponent for the homopolymer is always smaller than those for copolymers. The difference in the exponent γ for copolymers and that of the homopolymers increases as the difference in the energy of adsorption of the segments ($\mathcal{A}$ and $\mathcal{B}$) increases.

For the second definition of the thickness T, we use the polymer length ℓ, its fraction in loops f_{loop} and its average number of loops $\langle N_{loop} \rangle$. It is defined as follow:

$$T = \ell \, f_{loop} \, / \, (\, 2 \, \langle N_{loop} \rangle \,) \, . \tag{8}$$

The factor of two in the demominator appears because in every loop about a half of the segments are for going up and a half for going down. The results are shown in the log-log scale in figure 12b. Different from the Z_{max}, the thickness T obeys a power law very nicely ($c\ell^{\mu}$). As the repulsion of the $\mathcal{B}$ segments on the surface increases, the height of the loops increases and the adsorbed layer becomes more sparse (Fig. 4a). In this case the $\mathcal{A}$ segments are the ones that favor the loop formation due to the fact that this type of segments is attracted to the surface while the $\mathcal{B}$ is repelled. The μ exponents in this case are $\mu_{CRL} = 0.43$, $\mu_{SQR} = 0.54$, and $\mu_{TRI} = 0.79$. As a reference we may mention that the μ exponent in the homopolymer case is 0.51 [19]. The exponent μ seems to be more sensitive to the changes of the energy of interactions than the γ exponent. It is important to notice that in the homopolymer case the exponents γ and μ (for the Z_{max} and T respectively) are very similar numerically. However, in the copolymer case the equality in the exponents γ and μ seems to be broken.

It is important to mention that some recent Monte Carlo Simulations (MCS) [25] on random and alternating copolymers of two components with $\ell = 33$ give for Z_{max} an average layer thickness of 5.5 (in units of the lattice constant) for a case similar to our CRL calculation. When we compare Z_{max} from the MCS with the one we obtain from our simulation, we find that Z_{max} from MCS is a little smaller than the value in our case, $Z_{max} = 6.2$, for copolymers with the same length. The surface coverage (θ) values are practically the same in both simulations, $\theta_{MCS} = 0.59$ and 0.56 for alternating and randon copolymers, respectively, and $\theta_{CVM} = 0.61$ in our case. The small differences between them may be due to the polydispersity of the sample in our case. This agreement indicates that both MCS and the CVM simulations predict mostly the same behavior for this type of systems. In general in our model we observe that the repulsion of $\mathcal{B}$'s away from the surface enhances the height of the polymer film [21, 25]. Similar results have been observed by Marques and Joanny in the case of copolymers with a few $\mathcal{A}$

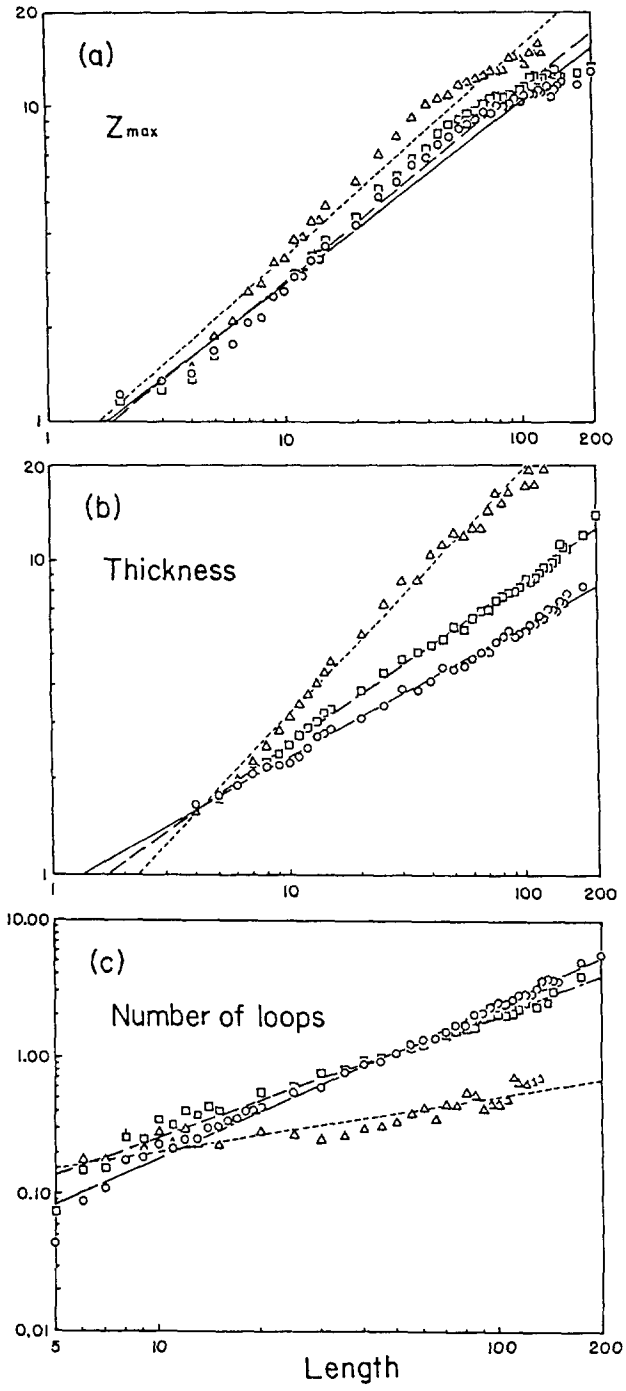

Fig. 12. — Some of the geometrical properties of the adsorbed copolymers as functions of the length (ℓ): a) Z_{max}, b) thickness T, and c) the average number of loops $\langle N_{loop} \rangle$. The marks correspond to the simulation output.

stickers regularly distributed along the chains [37].

The number of loops of the adsorbed chains also gives us information on the conformations adopted by the polymers. The average number of loops ($\langle N_{\text{loop}} \rangle$) in the log-log scale are show in figure 12c. The number of loops follow approximately a power law ($c\ell^{\kappa}$). The result shows that the number of loops is big in the case when the height of the loop is low (Fig. 12b), and *vice versa*. The exponents are $\kappa_{\text{CRL}} = 1.12$, $\kappa_{\text{SQR}} = 0.90$, and $\kappa_{\text{TRI}} = 0.41$, the results indicate that as the repulsion in the $\mathcal{B}$ increases the κ exponent decreases, therefore the number of loops decreases. When we compare the κ exponent in the copolymer case with the homopolymer case [19], the κ in the homopolymer (1.57) is bigger than in any of the copolymers we worked with. When the number of loops is smaller than one, this number can be interpreted as the fraction of copolymers that at least have one loop.

It has been pointed out that in many of the experimental data the thickness of the adsorbed polymer layer depends on the technique used in the measurement [6, 42-44]. Different experimental techniques give information about different aspects of the layer thickness: hydrodynamic layer thickness from hydrodynamics measurements and static layer thickness from static measurements. The experimental data indicate that the hydrodynamic thickness is always larger than the thickness determinated by the static techniques [6, 42-44]. In particular a very interesting observation was made by Cosgrove and coworkers who found that the profile measured by the small angle neutron scattering vanished completely at a distance which is about half of the hydrodynamics thickness. Cosgrove's observation supports the idea that the adsorbed polymer layer has two parts; a dense part close to the solid surface and a sparse part (sponge like) at the top of the dense part. The dense part of the layer thickness may be related to the static measurements while the outermost (exterior) may be related to the hydrodynamic measurements. Since in our simulation results the thickness T is related to the average height of the loops, we associate this with the dense part of the adsorbed layer while $Z_{\max}$ which is related to the farthest polymer segment is interpreted as the hydrodynamic layer thickness. For the purpose of comparing our results with the experimental observation made by Cosgrove, we calculate the following ratio:

$$C = \frac{\mathrm{T}}{Z_{\max}} \tag{9}$$

The C gives us qualitative information about the structure of the adsorbed polymer layer; there are three cases as is illustrated in figure 13a. *i*) When $C < 1$ the adsorbed polymer layer has two parts, a dense part close to the solid surface composed mainly of loops and trains and a sparse part (sponge like) at the top of the dense part composed mainly of tails; the energy is the leading factor in this type of conformations. *ii*) When $C \simeq 1$ the adsorbed polymer layer is made of just one compact *uniform* stratum like a step function near the surface, in this stratum we have mixing of trains, tails and loops; there is a balance between the energy and the entropy. *iii*) When $C > 1$ the adsorbed polymer layer is made of just one very sparse stratum, made of few very large loops with much meandering close to the surface and/or very long tails; the entropy takes over the energy in this case. It is important to notice that in the last case ($C > 1$) due to the meandering around of the loops near the surface T is larger than $Z_{\max}$ in equation (9). The results for the CRL and SQR indicate in figure 13b that for a very short polymer length there is a balance between the energy and the entropy, and as the length increases the energy dominates the process and C decreases gradually until $\ell \simeq 60$ where it reaches a very shallow minimum, beyound which the entropy takes over the energy part and C increases very slowly. In the TRI case due to the weak adsorption the entropy dominates in the whole range of the polymer length. The fluctuations in the TRI case are due to the reduced number of polymers used in the simulation; the fluctuation vanishes as we increase

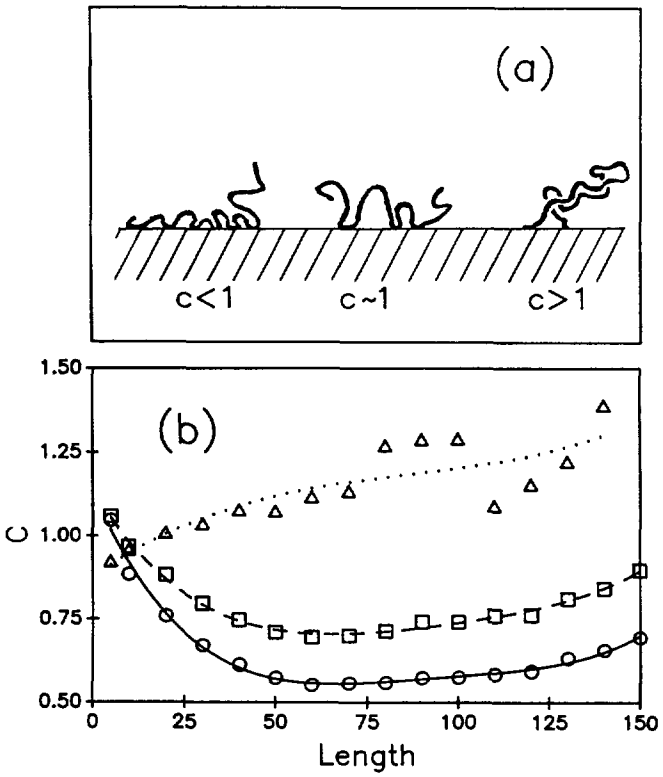

Fig. 13. — a) Three possible cases for the C ratio. b) The simulation results for the C ratio as a function of the polymer length (ℓ). The lines are aid to the eye.

the number of polymers used in counting. We cannot answer the question whether or not the C ratio keeps on growing or levels off as the polymer length increases, because our simulation results are limitated to a finte length range.

We calculate the area covered by the adsorbed copolymers. The area we call $A_{\max}$ is the rectangular area that circumscribes the copolymer segments on the $n = 1$ plane for every adsorbed copolymer chain, and we take the average for all chains with the same length ℓ. The results of this calculation in units of square lattice constants are shown on the log-log scale in figure 14. The results show clearly that $A_{\max}$ follows a power law ($c\ell^{\delta}$) very nicely in all cases. The exponents δ are 1.23, 1.12 and 0.65 for the CRL, SQR and TRI, respectively. The results are as expected, the area decreases as the repulsion increases. The exponents δ in these cases are smaller than the one in the homopolymer case ($\delta = 1.42$). The results shown in figures 12 and 14 suggest that in most of the cases the exponents of the power law are very sensitive to the surface interactions.

We can get more information about the conformation and its variation with the copolymer length using $A_{\max}$ and $Z_{\max}$. We calculate the following ratio:

$$R = \frac{\sqrt{A_{\max}}}{Z_{\max}} \tag{10}$$

This R gives us information about the lateral view of the adsorbed copolymers; there are three cases as illustrated in figure 15a. *i*) When $R < 1$, a small part of the adsorbed polymer touches

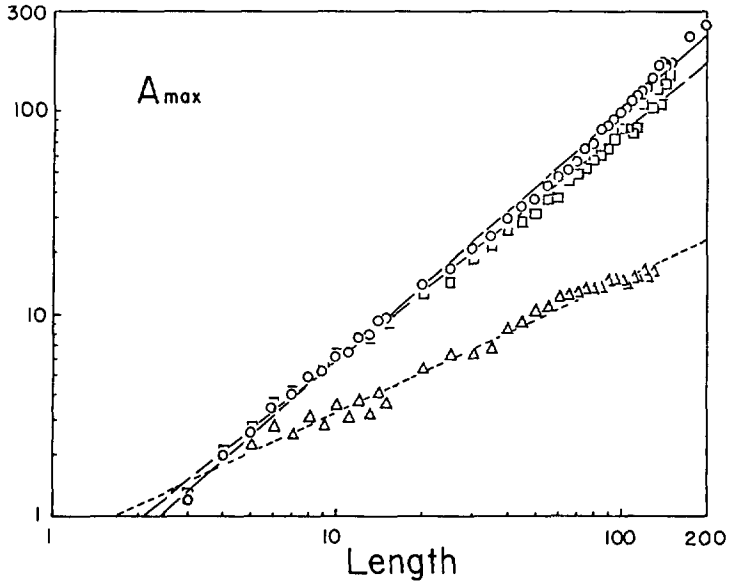

Fig. 14. — The maximum rectangular area A_{max} covered by the adsorbed copolymers as a function of the length (ℓ).

the surface and the rest of the body is mainly extended into the solution. The polymer can be contained in a vertical rectangle, and the entropy effect is more important than the energy effect in this case. *ii*) When $R \simeq 1$, the adsorbed polymer can be contained in a square, and there is a balace between the entropy and the energy contribution and both effects are important. *iii*) When $R > 1$, the adsorbed polymer is mainly kept close to the surface and the polymer can be contained in a horizontal rectangle, so that in this case the energy effect is more important than the entropy effect. In figure 15b we show the result of our simulation. In the CRL and SQR cases the R presents a very shallow minimum due to the competition between the entropy and energy effect, this minimum corresponding to the point where the energy contribution takes over the entropy contribution. For this reason the R begins to go up for copolymers whose length are above this point ($\ell \simeq 50$). This observation is in agreement with the results presented for Z_{max} in figure 12a that suggest a change in the conformation of the adsorbed copolymers with the length. Whether the R ratio in the CRL and SQR cases continue to increase with the length or levels-off, we cannot answer because of the limited range of length studied here. In the TRI case, due to the weak energy of adsorption, the entropy has a major role than the energy. The low R values indicate that the conformations adopted by the adsorbed copolymers are mainly extended into the bulk (away from the surface). The result suggests that in the TRI case the R ratio levels off for very long copolymers. These results suggest a way to tailor the copolymers to obtain specific conformations in the adsorbed layer.

It is also informative to examine the evolution of the fractions in trains, tails and loops as the repulsion of the $\mathcal{B}$ monomers changes. The fractions are shown in figure 16a, b and c for the CRL, SQR and TRI, respectively. The results indicate that in the case of short polymers the fraction values do not depend much in the repulsion of the $\mathcal{B}$ segments, because there are only a few $\mathcal{B}$'s in short chains as is shown in figure 3. The differences in the behavior in the fractions become noticeable for chains with $\ell \geq 10$. The train fraction decreases as the repulsion of the $\mathcal{B}$ segments increases as shown in (a), (b) and (c). For a given interaction of the $\mathcal{B}$ segments

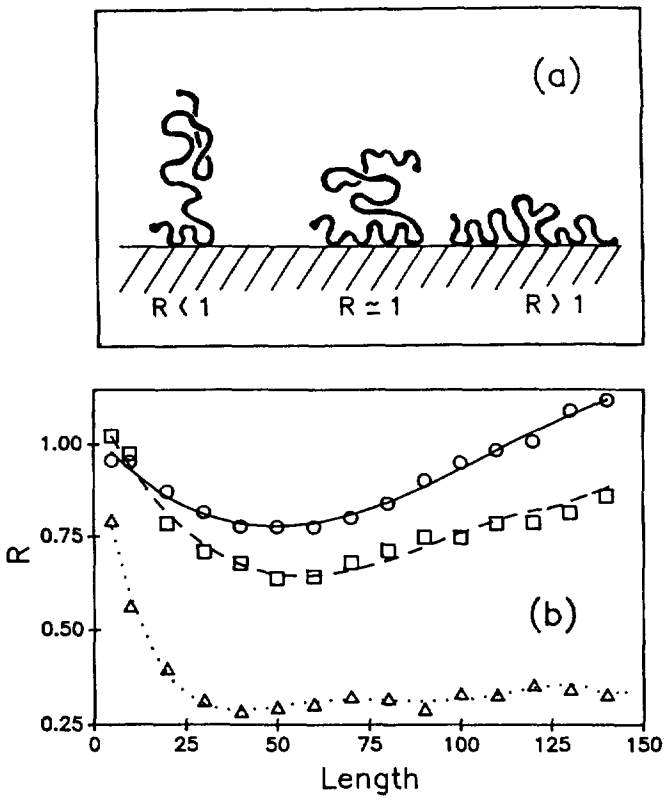

Fig. 15. — a) Three possible cases for the R ratio. b) The simulation results for the R ratio as a function of the polymer length (ℓ). The lines are aid to the eye.

the train fraction decreases as the the polymer length increases and later the fraction levels off. As the $\mathcal{B}$ interaction changes, the train fraction for long polymers changes from 0.27 in the CRL to 0.035 in the TRI case. The tail fraction for a given $\mathcal{B}$ interaction increases with the length, goes through a maximum when the repulsion is not very strong (CRL and SQR), and later decreases and levels off. For the strong repulsion (TRI) the maximum seems to disappear and only the leveling off behavior is shown. When we look at the tail fraction through the series (a) to (c), it is clear that the repulsion changes the copolymer conformations drastically. For very long copolymers the dominance of the tail fraction is noticeable in (c), while the three curves are almost the same in (a). The loop fraction for a given repulsion of $\mathcal{B}$ increases with the polymer length. The loop fraction as a funcion of the repulsion of the $\mathcal{B}$ segments increases slightly, but after some value the loop fraction begins to decrease.

The evolution of the number of tails as a function of the polymer length is presented in figure 17. Since the polymers studied here are linear polymers with no branching, the number of tails can be zero, one or two as is illustrated in figure 11. The results are presented in figures 17a, b and c for CRL, SQR and TRI, respectively, in the increasing order of the $\mathcal{B}$ repulsion. The fraction of adsorbed polymers with zero tails for a given interaction decreases with the polymer length. The fraction of polymers adsorbed with one tail for a given interaction increases with the length, goes through a maximum and later levels off. When the repulsion of the $\mathcal{B}$ segments increases the fraction with one tail increases and becomes the dominant

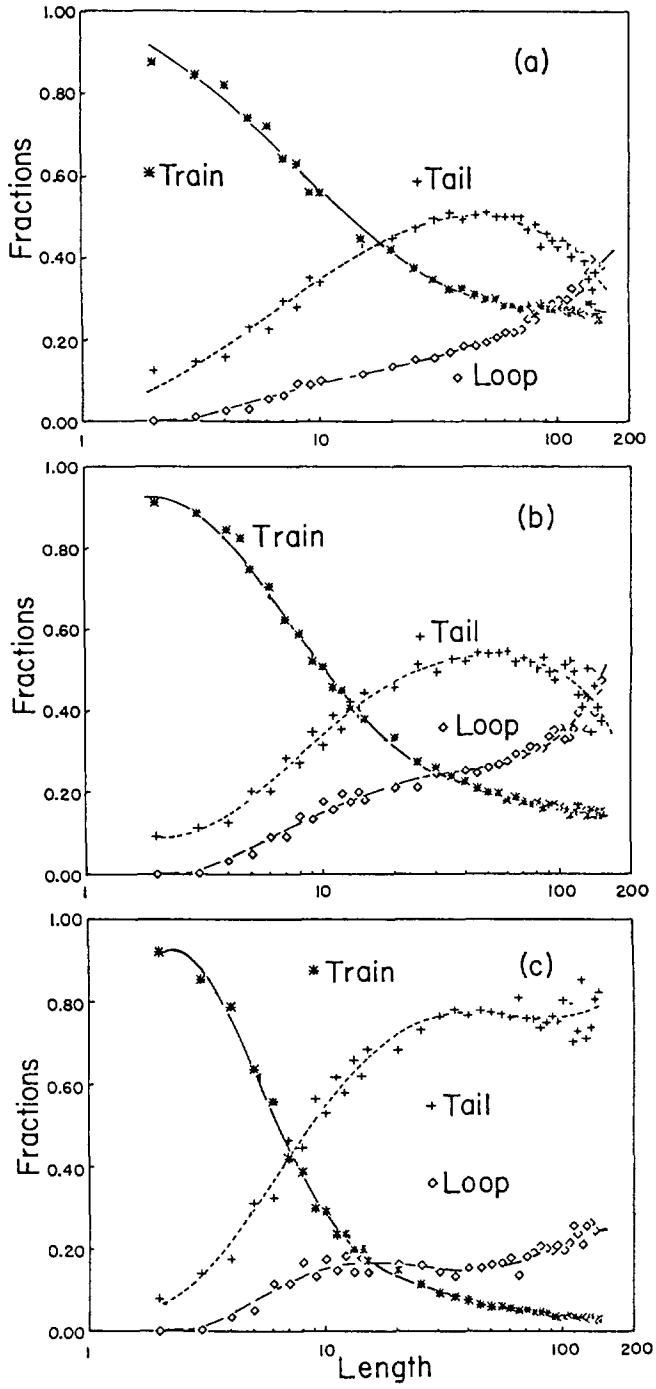

Fig. 16. — The fractions in train, tail and loop of the adsorbed copolymers as functions of the length (ℓ). a) CRL, b) SQR and c) TRI. Lines are an aid to the eye.

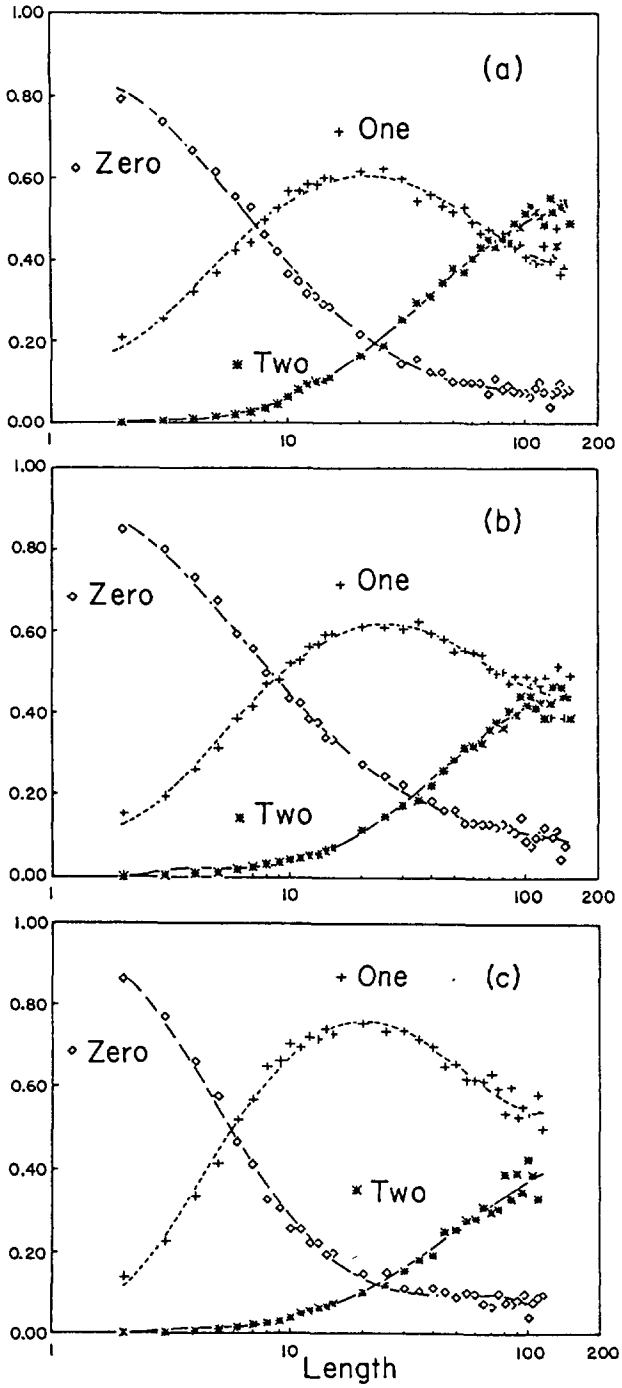

Fig. 17. — The fractions with zero, one and two dangling tails for the adsorbed copolymers as functions of the length (ℓ). a) CRL, b) SQR, and c) TRI. Lines are aid to the eye.

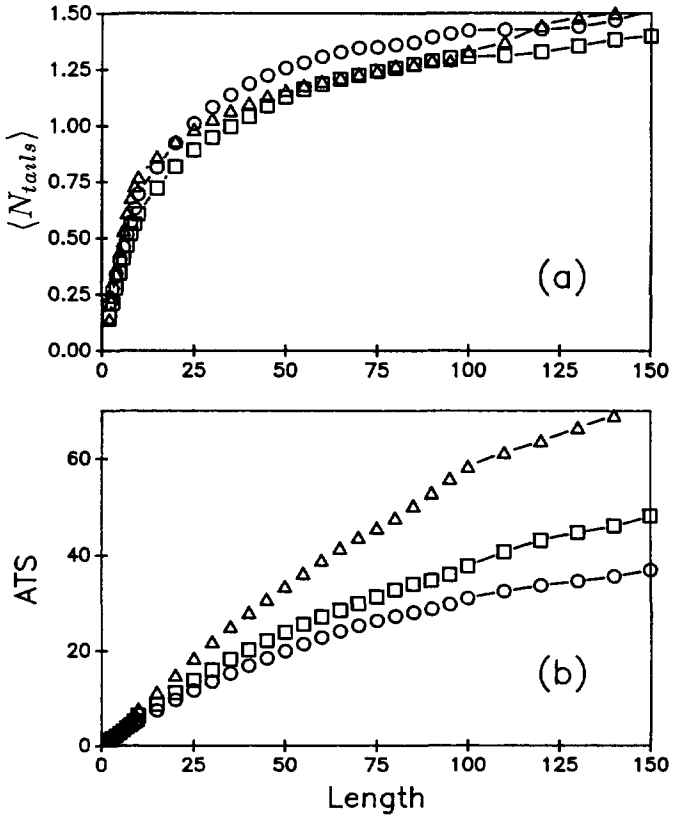

Fig. 18. — a) Simulation results for the average number of tails $\langle N_{\text{tails}} \rangle$ per polymer as a function of the polymer length for the CRL, SQR and TRI cases. b) Simulation results for the average tail size (ATS) per adsorbed polymer as a function of the polymer length for the CRL, SQR and TRI cases.

fraction. The fraction with two tails for a constant $\mathcal{B}$ interaction increases with the length and later levels off. When the repulsion with the surface is larger, this fraction is smaller in the entire range of lengths.

It is of interest to calculate the average number of tails ($\langle N_{\text{tails}} \rangle$) per chain based on the results presented in figure 17. The results of this calculaton are in figure 18a. From the results in figure 18a we can see that the conformations adopted by the copolymers in the three cases are such that they have approximately the same number of tails for the three cases. The $\langle N_{\text{tails}} \rangle$ increases as the copolymer length increases, approximately approaching 1.5 for the case of the largest copolymers presented here.

Since many authors have pointed out the importance of the tails in the hydrodynamic thickness [6, 17, 42-44], we calculate the Average Tail Size (ATS) per polymer using the following definition:

$$\text{ATS} = \frac{\ell \, f_{\text{tail}}}{\langle N_{\text{tails}} \rangle} \, . \tag{11}$$

where f_{tail} is the average tail faction in every copolymer (see Fig. 16). The results of this calculation shown in figure 18b are as expected; the largest ATS value corresponds to the TRI

case. In this case there is a large entropy contribution due to the meandering of the long tails. As the repulsion of the $\mathcal{B}$ segments decreases, the ATS decreases and the energy contribution makes the copolymer conformation more flat for the SQR and CRL cases.

4. Comparison with experimental work.

The comparison with experimental work seems difficult at this moment. However, there are two possible candidates for comparison of the model with the experimental results: *i*) the copolymers of polyethylene oxide (PEO) and polypropylene oxide (PPO), and *ii*) the copolymers of poly(vinylpyridine) (PVP) and polystyrene (PS). The PPO (PVP) segments show a hydrophobic behavior, and the PEO (PS) segments show a hydrophilic behavior in the similar way as our $\mathcal{A}$ and $\mathcal{B}$ segments, respectively. The PEO-PPO copolymers can be used for comparison. This copolymer is named commercially Ucons. There are some evidence that Ucons are random (statistical) copolymers [9]. This makes it an possible candidate for comparison with the theory. However, we did not find information of the configurations adopted by Ucons when they are adsorbed on the surfaces. The only information about the configurations we found says that they are adsorbed with configurations that promote the train, tail and loop formation [9]. For the PVP-PS copolymers most of the experimental results [7, 8] are for diblock and triblock copolymers rather than a statistical copolymer. We did not find any experimental work for statistical copolymers of PVP-PS.

Acknowledgments.

One of the authors (FAG) cordially acknowledge the Consejo Nacional de Ciencia y Tecnología (CONACyT, México) Grant 1774-E9210.

References

[1] van der Linden C. and van Leemput R., *J. Colloid Int. Sci.* **67** (1978) 48.

[2] van der Linden C. and van Leemput R., *J. Colloid Int. Sci.* **67** (1978) 63.

[3] Kayes J.B. and Rawlins D.A., *Colloid Polym. Sci.* **257** (1979) 622.

[4] Kawaguchi M., Hayakawa K. and Takahashi A., *Polymer J.* **12** (1980) 265.

[5] Takahashi A. and Kawaguchi M., *Ad. Polym. Sci.* **46** (Springer Verlag, Berlin Heidelberg, 1982) 1.

[6] Cohen Stuart M.A., van der Boongaard Th., M. Zourab Sh. and Lyklema J., *Colloids Surf.* **9** (1984) 163.

[7] Tirrell M., Patel S. and Hadziioannou G., *Proc. Natl. Acad. Sci. USA* **84** (1987) 4725.

[8] Patel S., Tirrell M. and Hadziioannou G., *Colloids Surf.* **31** (1988) 157.

[9] Baker J.A. and Berg J.C., *Langmuir* **4** (1988) 1055.

[10] Cesarano III J., Ph.D. Thesis, University of Washington, U.S.A. (1989).

[11] Roe R.J., *J. Chem. Phys.* **60** (1974) 4192.

[12] Scheutjens J.M.H.M. and Fleer G.J., *Discuss. Faraday Soc.* **65** (1978) 221.

[13] Scheutjens J.M.H.M. and Fleer G.J., *J. Phys. Chem.* **83** (1979) 1619.

[14] Scheutjens J.M.H.M. and Fleer G.J., *J. Phys. Chem.* **84** (1980) 178.

[15] Scheutjens J.M.H.M., Ph.D. Thesis, Agricultural University, Wageningen, the Netherlands (1985).

[16] Papenhuijzen J., van der Schee H.A. and Fleer G.J., *J. Colloid Int. Sci.* **104** (1985) 540.

[17] Fleer G.J., Scheutjens J.M.H.M., Cohen Stuart M.A., *Colloids Surf.* **31** (1988) 1.

[18] Aguilera-Granja F. and Kikuchi R., *Physica A* **189** (1992) 81.

[19] Aguilera-Granja F. and Kikuchi R., *Physica A* **189** (1992) 108.

[20] Aguilera-Granja F. and Kikuchi R., *Mat. Res. Soc. Symp. Proc.* **153** (1989) 163.

[21] Aguilera-Granja F. and Kikuchi R., Adsorption of polymers on surfaces, Lectures on Thermodynamics and Statistical Mechanics, M. López de Haro and C. Varea Eds. (Published by World Scientific, 1990) pp. 141-154.

[22] Shih W.Y., Shih W.H. and Aksay I.A., *Mat. Res. Soc. Symp. Proc.* **140** (1989) 431.

[23] Balazs A.C. and Lewandowski S., *Macromolecules* **23** (1990) 839.

[24] Balazs A.C., Huang K. and Lantman C.W., *Macromolecules* **23** (1990) 4641.

[25] Balazs A.C., Gempe M. and Lantman C.W., *Macromolecules* **24** (1991) 168.

[26] Huang K., Balazs A.C., *Phys. Rev. Lett.* **66** (1991) 620.

[27] Balazs A.C., Gempe M.C. and Zhou Z., *Macromolecules* **24** (1991) 4918.

[28] Aguilera-Granja F. and Kikuchi R., *Physica A* **195** (1993) 53.

[29] Aguilera-Granja F. and Kikuchi R., *J. Phys. II France* **3** (1993) 1141.

[30] Pincus P., Interaction Between Polymers and Colloidal Particles, *Lectures on Thermodynamics and Statistical Mechanics*, A. E. González and C. Varea Eds. (published by World Scientific, 1988).

[31] Aguilera-Granja F. and Kikuchi R., *Physica A* **176** (1991) 514.

[32] Aguilera-Granja F. and Kikuchi R., *Physica A* **182** (1992) 331.

[33] Kikuchi R., *Phys. Rev.* **81** (1951) 988.

[34] Kikuchi R., *Phys. Rev. B* **22** (1980) 3784.

[35] de Gennes P.G., *Macromolecules* **14** (1981) 1637.

[36] de Gennes P.G. and Pincus P., *J. Phys. Lett.* **44** (1983) L-241.

[37] Marques C.M. and Joanny J.F., *Macromolecules* **23** (1990) 268.

[38] Eisenriegler E., Kremer K. and Binder K., *J. Chem. Phys.* **77** (1982) 6296.

[39] Bouchaud E. and Daoud M., *J. Phys. France* **48** (1987) 1991.

[40] Fisher M., *J. Phys. Soc. Jpn* **26** (1969) 44.

[41] de Gennes P.G., Scaling Concepts in Polymer Physics (Cornell University Press: Ithaca, NY, 1979).

[42] Scheutjens J.M.H.M., Fleer G.J. and Cohen Stuart M.A., *Colloids Surf.* **21** (1986) 285.

[43] Cohen Stuart M.A., Waajen F.H.W.H., Cosgrove T., Vincent B. and Crowley T.L., *Macromolecules* **17** (1984) 1825.

[44] Cosgrove T., Vincent B., Crowley T.L. and Cohen Stuart M.A., *ACS Symp. Ser.* **240** (1984).